

Templated Growth of Carbon Nanotubes on Nickel Loaded Mesoporous MCM-41 and MCM-48 Molecular Sieves

M. Masoumi¹, M. R. Mehrnia^{1*}, M. M. Montazer-Rahmati¹, A. M. Rashidi²

1- School of Chemical Engineering, University College of Engineering, University of Tehran, Tehran, I. R. Iran

2- Gas Division, Research Institute of Petroleum Industry (RIPI), Tehran, I. R. Iran

(*) Corresponding author: mmehrnian@ut.ac.ir

(Received: 02 Feb. 2010 and Accepted: 30 Apr. 2010)

Abstract:

Chemical vapor deposition was employed to synthesize carbon nanotubes with Ni-loaded MCM-41 and MCM-48 as catalysts and acetylene as precursor at 750°C. Mesoporous Ni MCM-41 and Ni MCM-48 molecular sieves were synthesized by a hydrothermal method and were characterized by XRD and N₂ adsorption isotherm. The catalytically synthesized carbon materials were characterized with Raman spectroscopy, N₂ adsorption isotherm, SEM and TEM. The experimental results indicated that the deposited carbon materials by acetylene decomposition were slightly more in the Ni MCM-41 framework than in Ni MCM-48. Furthermore, the diameter distribution of the well-ordered grown multi wall carbon nanotubes has direct relation with their silicate frameworks.

Keywords: Nano structures, Chemical vapor deposition, Electron microscopy, Mesoporous structure

1. INTRODUCTION

Carbon nanotubes (CNTs) have high mechanical strength, thermal conductivity and unique electronic properties. Several efforts have been made to control the metallic particles for CNTs growth with controllable diameter and well-oriented structures. The key point to the control the growth of CNTs is to control the similar metal clusters in catalysts, avoiding the aggregation of these clusters into large particles during the high temperature reaction [1]. In recent years, some papers have been published on the synthesis of carbon nanotubes in microporous molecular sieve zeolites as the catalyst supports [2-7].

Zeolites are crystalline microporous materials which are widely used as catalysts in oil refining,

petrochemistry and organic synthesis. Also they have been used as adsorbents and ion-exchange media [6,7]. Recently, there has been growing interests in the synthesis of new molecular sieves extending the pore diameter to the mesoporous region. The mesoporous molecular sieves are obtained with various structures and pore diameters that can be controlled over a wide range (1.6-50 nm) [6,8]. It is well known that different catalyst supports would strongly influence the catalytic properties due to the different interactions between the catalyst particles and supports. Mesoporous molecular sieves such as MCM-41 and MCM-48 materials are the kinds of new catalyst supports with many interesting properties [7]. Therefore, they have seldom been used to date in the synthesis of CNTs on metal loaded M41S and

some arguments on this aspect have appeared. The aim of the present work was to study the synthesis of multi wall carbon nanotubes (MWNTs) on the nickel loaded mesoporous MCM-41 and MCM-48 catalysts. Moreover, the pore size distributions of synthesized CNTs were related to the silicate support framework of synthesized catalysts.

2. EXPERIMENTAL

2.1. Preparation of Ni loaded mesoporous silicates

Sodium meta silicate, cetyl trimethyl ammonium bromide (CTAB) and nickel nitrate were respectively used as the sources of silica, structure directing agent and nickel. The Ni-loaded MCM-41 was synthesized as follows: First, 20.2 g of CTAB was dissolved in 120 ml of distilled water with stirring and slightly warming. In addition nickel nitrate was dissolved in 120 ml distilled water and 49.3 g of sodium meta silicate was added to this solution until a colloidal solution with molar ratio of Si/Ni=20 was prepared. Next, this solution was stirred and slightly warmed for 30 minutes in order to prepare a homogenous solution. When the homogenous solution was prepared, the solution of CTAB in the distilled water was added to that solution and stirred again for 30 minutes to prepare the initial reacting mixture. After that the reacting mixture was transferred into the autoclave and heated at 100°C for 72 hours, then, 400 ml of 70% ethanol and 10 ml of 37% HCl were added to the sample and stirred slightly for 30 minutes. After that the crystalline materials were separated by filtration and washed with distilled water and dried at 120°C for 4 hours.

In addition, in order to synthesize the Ni-loaded MCM-48, 14 g of CTAB was dissolved in 120 ml of distilled water by stirring and slight warming. Also 42 g of sodium meta silicate was dissolved in 120 ml of distilled water and the homogenous solution of nickel nitrate and sodium meta silicate with a molar ratio Si/Ni = 20 was prepared as previously mentioned. After that, for preparation of the initial reacting mixture, the solution of CTAB in distilled water was added to the homogenous solution and

stirred again for 30 minutes, and then, the final mixture was transferred into the autoclave and was crystallized at 100°C for 72 hours. When the crystallization period was completed, the autoclave was cooled and the crystalline Ni MCM-48 materials were discharged and treated with the similar method which was used for Ni MCM-41.

The final active Ni MCM-41 and Ni MCM-48 catalysts were obtained by removing the occluded surfactant, which fills the pores by calcinating the samples at 550 °C in air for 6 hours. After the calcination process, some white materials were obtained.

2.2. Preparation of CNTs

The catalytic reactions for the synthesis of CNTs were carried out using the synthesized Ni MCM-41 and Ni MCM-48 as the catalysts. The Chemical vapor deposition (CVD) technique was carried out in a horizontal furnace consisting of a quartz tube with a diameter of 45 mm and 1 m in length. The furnace provided controllable heating up to 1200°C with a non-gradient temperature zone (reaction zone) of 30 cm in length. At first, 1 g of the catalyst was placed in a quartz boat that was placed into a quartz tube. Then, the catalyst was purged in a hydrogen stream at a flow rate of 300 ml/min for 30 min in order to reduce the catalyst. After that, the reaction was carried out using acetylene as the carbon source with a flow rate of 30 ml/min and hydrogen as carrier gas with a flow rate of 300 ml/min at 750°C for 30 min. 750 °C was found to be the suitable temperature to achieve the high yield of carbon deposition. Finally, the furnace was cooled at room temperature under a hydrogen atmosphere and black materials formed as the final product after completion of the reaction.

2.3. Purification of synthesized carbon nanotubes

The synthesized materials were purified as follows. In order to obtain pure carbon nanotubes, silicate components were removed by dissolving in 47% HF solution, and this stage was carried out for about 10 min. HF-treated samples were washed several times with distilled water, and the washing process continued until neutral materials were obtained. Then, to remove residual metallic nickel particles,

CNTs were treated with a 2 M HCl solution for 120 min. After that, the washing step was repeated as mentioned above for the HF treatment process, and treated CNTs were dried at 100°C. Finally, in order to eliminate amorphous carbons, all of the synthesized materials (CNTs and CNTs/Ni M41S) were placed in the furnace at 400°C for 120 min.

2.4. Characterization of the synthesized materials

The powder XRD patterns of the calcined mesoporous Ni MCM-41 and Ni MCM-48 molecular sieves were obtained with a Philips PW1848 diffractometer using nickel-filtered Cu K α radiation ($\lambda = 0.154$ nm). The diffractograms were recorded in the 2θ range of 0–10° in the steps of 0.02° with a count time of 15 sec at each point. The surface area, pore volume and pore size distribution were measured by nitrogen adsorption at 77 K using an ASAP-2010 porosimeter from the Micromeritics Corporation GA. The samples were degassed at 350 °C and 1.33-0.67 kPa overnight prior to the adsorption experiments. The pore size distribution (PSD) was evaluated from the adsorption isotherms using the Barrett, Joyner and Halenda (BJH) algorithm (ASAP-2010) available as a built-in software from Micromeritics. Spectra were collected with a Renishaw Ramanscope in the backscattering configuration using 514.5 nm laser wavelengths. Scanning Electron Microscopy (SEM) images using a Camscan MV2300 Microscope with an operating voltage of 15 kV and Transmission Electron Microscopy (TEM) images using a JEOL 1200 EXII microscope with an operating voltage of 100 kV were obtained in the present work to verify the desired structure of the synthesized nanotubes.

3. RESULTS AND DISCUSSION

The X-ray diffractograms of the calcined Ni MCM-41 and Ni MCM-48 are shown in Figures 1 and 2.

The powder XRD patterns of the prepared Ni MCM-41silica sample (Figure 1) exhibit reflections [100], [110] and [200] planes in a small-angle range of $2\theta=2-8^\circ$ [9], which is characteristic of the hexagonal ordered structure and suggests that the MCM-41 mesoporous materials have good thermal stability after calcination. The calcined material shows strong signal between 1.8 and 2.8° (2θ), due to the [100] reflection plane and weak signals between 3.8° and 4.8° (2θ), and due to the higher order [110] and [200] reflections indicate the formation of well-ordered mesoporous materials [10]. It also shows that our materials are well organized even after calcination.

The powder XRD patterns of the prepared Ni MCM-48 silica sample (Figure 2) also exhibit reflections [211] and [220] planes. The well-defined XRD pattern shows the typical $h k l$ reflections that can be indexed to cubic MCM-48 [6,11].

The activity of the synthesized catalysts of Ni MCM-41 and Ni MCM-48 molecular sieves was evaluated by measuring the deposition of carbon using equation 1 [12]. Results are presented in the Table 1.

$$\text{Carbon yeild (\%)} = \left(\frac{M_T - M_{Cat}}{M_{Cat}} \right) \times 100 \quad (1)$$

Where M_{Cat} is the weight of the catalyst taken before CNT growth, M_T is the weight of the catalyst and CNT grown on the catalyst.

In both catalysts carbon atoms can deposit on the metal surface. Carbon would diffuse on the metal surface that is situated in the crystalline structure of the M41S catalysts. As presented in Table 1, Ni is an effective catalyst that can be used for carbon nanotubes synthesis. The amount of carbon deposited on the Ni MCM-41 is greater than that deposited on Ni MCM-48. Paying attention to the structure of MCM-41 whose crystallites build up from hexagonally arranged tubes ($p6mm$), provides easier access to the Ni in MCM-41 structure for

Table 1: Carbon deposition yield on various Ni M41S catalysts

Catalyst	M_{Cat} (g)	M_T (g)	Carbon yield (%)
Ni MCM-41	1	1.42	42
Ni MCM-48	1	1.38	38

Table 2: N_2 adsorption data of Ni M41S catalysts

Catalyst	BET Surface Area (m^2/g)	Average Pore Diameter- by BET (nm)	BJH Adsorption Average Pore Diameter (nm)	BJH Adsorption Cumulative Pore Volume of Pores (cm^3/g)
Ni MCM-41	908.76	2.88	2.64	0.77
Ni MCM-48	1098.46	3.16	3.46	1.06

carbon atoms than the Ni in the MCM-48 structure with a cubic arrangement of mesopores building up a quasi three-dimensional pore system (cubic $Ia3d$) [9].

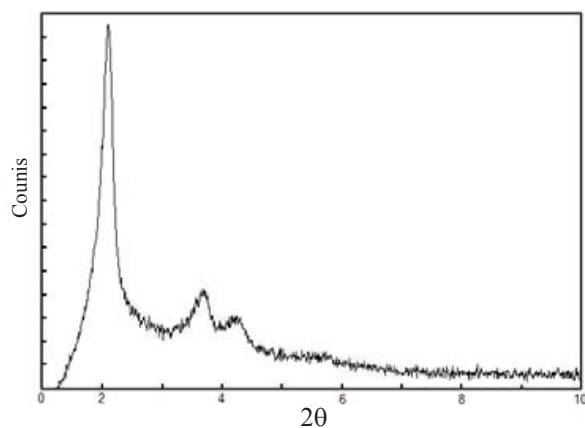


Figure 1: XRD pattern of Ni MCM-41.

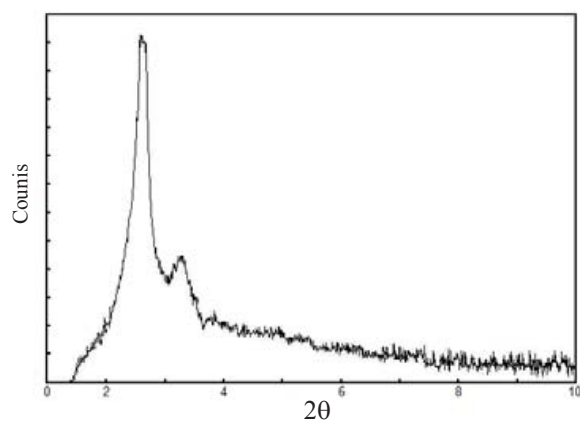


Figure 2: XRD pattern of Ni MCM-48.

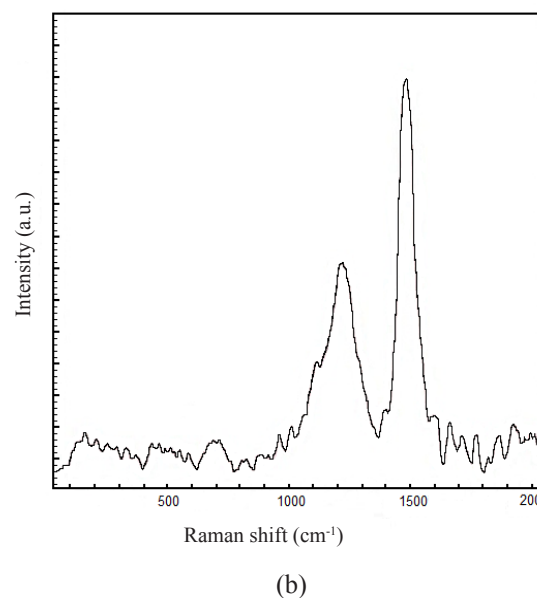
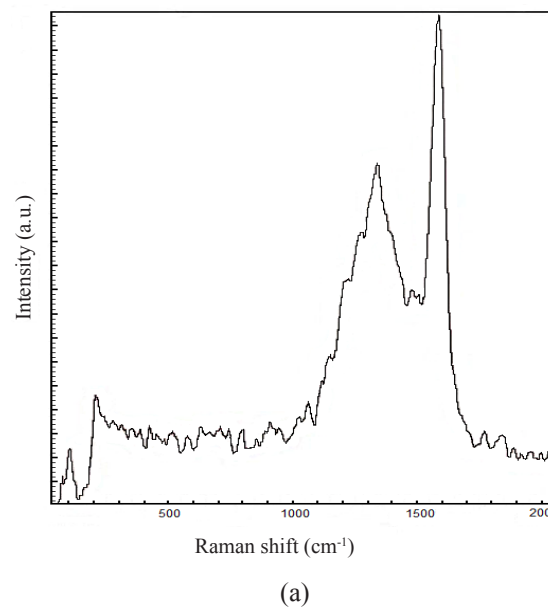
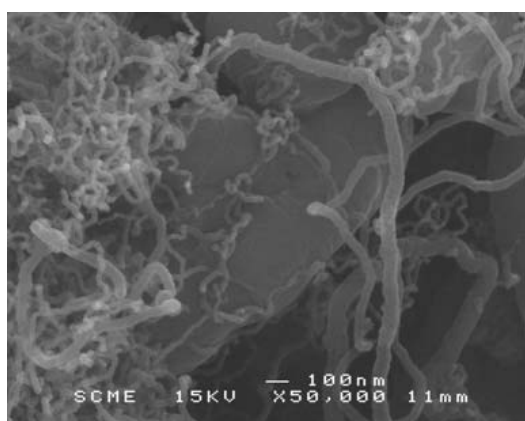
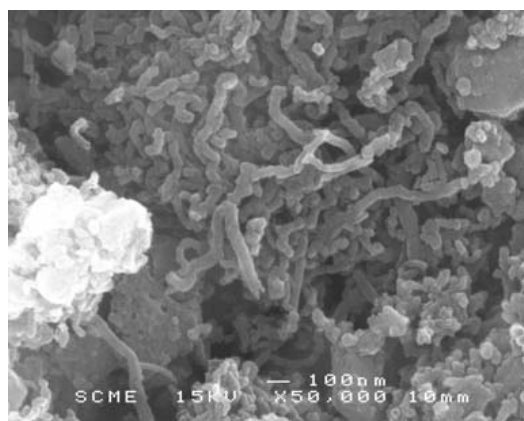


Figure 3: Raman spectrum of MWNTs grown over (a) Ni MCM-41 (b) Ni MCM-48.

In addition the presence of MWNTs in the sample prepared by the CVD method was confirmed by Raman spectroscopy. Because of the absence of the radial breathing mode (RBM) peak in the spectra,



(a)

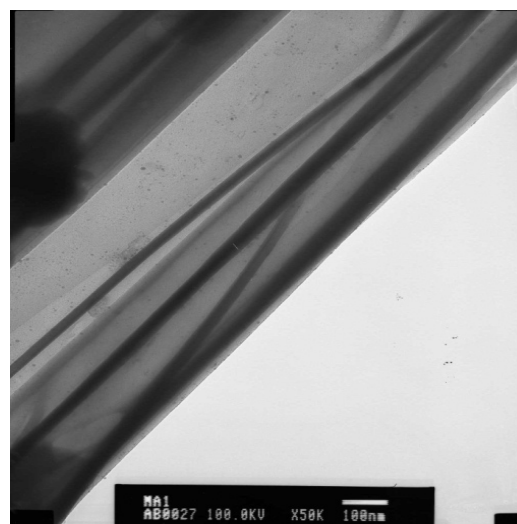


(b)

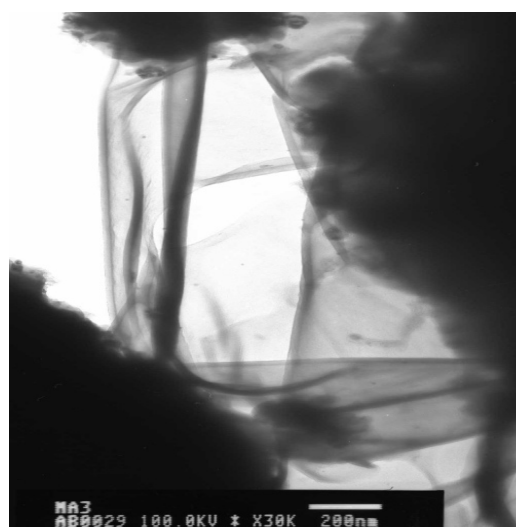
Figure 4: SEM image of CNTs grew on (a) Ni MCM-41 and (b) Ni MCM-48.

the most portions of the produced CNTs were MWNTs.

The first-order Raman spectrum typically between 1000 and 2000 cm^{-1} is composed of two intense peaks, at about 1350 and 1600 cm^{-1} . Figure 3(a) shows two major peaks at 1585 and 1340 cm^{-1} which corresponds to G-band and D-band, respectively, for the MWNTs grown on Ni MCM-41. Similarly, Figure 3(b) shows two peaks at 1597 and 1360 cm^{-1} for the MWNTs formed over the Ni MCM-48. The G-band observed at 1585 and 1597 cm^{-1} has been assigned to the Raman allowed phonon E_{2g} (stretching) mode of graphite. The strongest



(a)



(b)

Figure 5: TEM image of CNTs grew on (a) Ni MCM-41 and (b) Ni MCM-48.

peak of the G-band in the spectrum indicates the formation of good arrangements of the hexagonal lattice of graphite. The band at 1340 and 1360 cm^{-1} corresponds to the D-band. The relatively weak D-band in the spectra reveals the high purity and is assigned to the A_{1g} phonon [13]. The intensity ratio of the G band to the D band (I_G/I_D) can express the graphitization of carbon nanotubes [14,15]. High

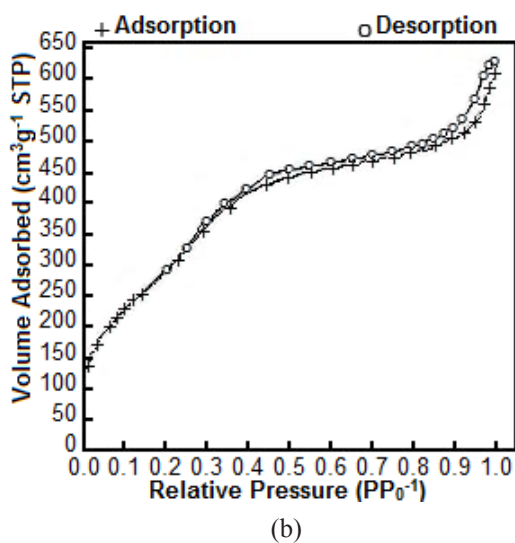
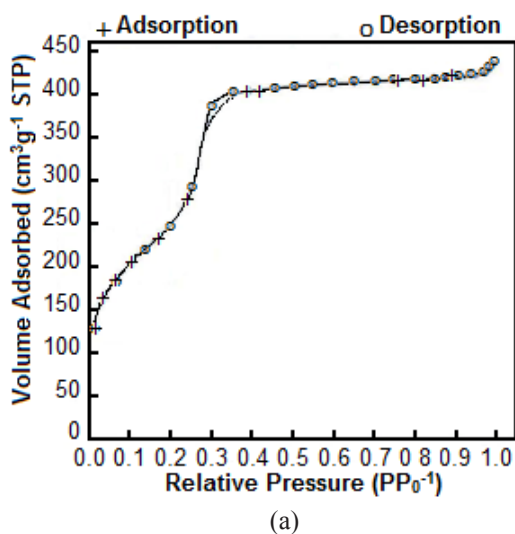


Figure 6: N_2 adsorption–desorption isotherms of (a) Ni MCM-41 and (b) Ni MCM-48

I_G/I_D value represents good graphitic structure of CNTs.

SEM images were obtained from CNTs with Ni MCM-41 and Ni MCM-48 at a magnification of 50,000 \times . The images show a cluster of CNTs adhered together. The images obtained from CNTs grown on Ni MCM-41 and Ni MCM-48 are shown in Figures 4(a) and 4(b), respectively. Individual CNTs were not resolved by the SEM images, but the CNTs appearing as the filaments are clearly seen.

These images also indicate the formation of carbon nanotubes on the outer surface of the mesoporous materials.

The TEM images of individual MWNTs grown on Ni MCM-41 and Ni MCM-48 are shown in Figures 5(a) and 5(b), respectively.

The TEM images of MWNTs show the tubular structure of MWNTs in the sample, and it was found that only a very small amount of amorphous carbon and other forms of carbon are presented in the sample. Also, Isolated MWNTs with clean tube walls are observed in the sample. The results revealed that the MWNTs are uniform in the range of 25–40 nm for the MWNTs grown over Ni MCM-41 and 25-30 nm for MWNTs grown over Ni MCM-48. The length of the tube was found to be in the micron range.

TEM image shows that MWNTs grew in a narrow-diameter range over Ni MCM-48. Similar diameter and the good alignment of MWNTs in both cases are due to the fact that the tubes follow the structure of their substrate framework. As can be seen MWNTs' growth follows a based-growth model because Ni clusters have strong interactions with M41S and are embedded in the nano-catalyst structure.

Table 2 presents the BET surface area, average pore size diameter and pore volume of the catalysts.

The results from table 2 show that all of the measured values by the N_2 adsorption method of Ni MCM-48 are greater than Ni MCM-41, which is in agreement with reports in the literature [16].

The results of both XRD and N_2 physisorption are complementary with respect to probing the structural integrity of Ni MCM-41 and Ni MCM-48. XRD analysis demonstrates the hexagonal structure of the Ni MCM-41 and the cubic structure of Ni MCM-48, while N_2 physisorption gives information about the extent of the uniformity of the mesopores. The N_2 adsorption–desorption isotherms and PSD of Ni MCM-41 and Ni MCM-48 are respectively shown in Figures 6(a) and 6(b) and Figures 7(a) and 7(b). The isotherms of all samples show a sharp inflection step at p/p_0 of ≈ 0.3 – 0.4 , characteristic of capillary condensation of uniform mesoporous materials. The

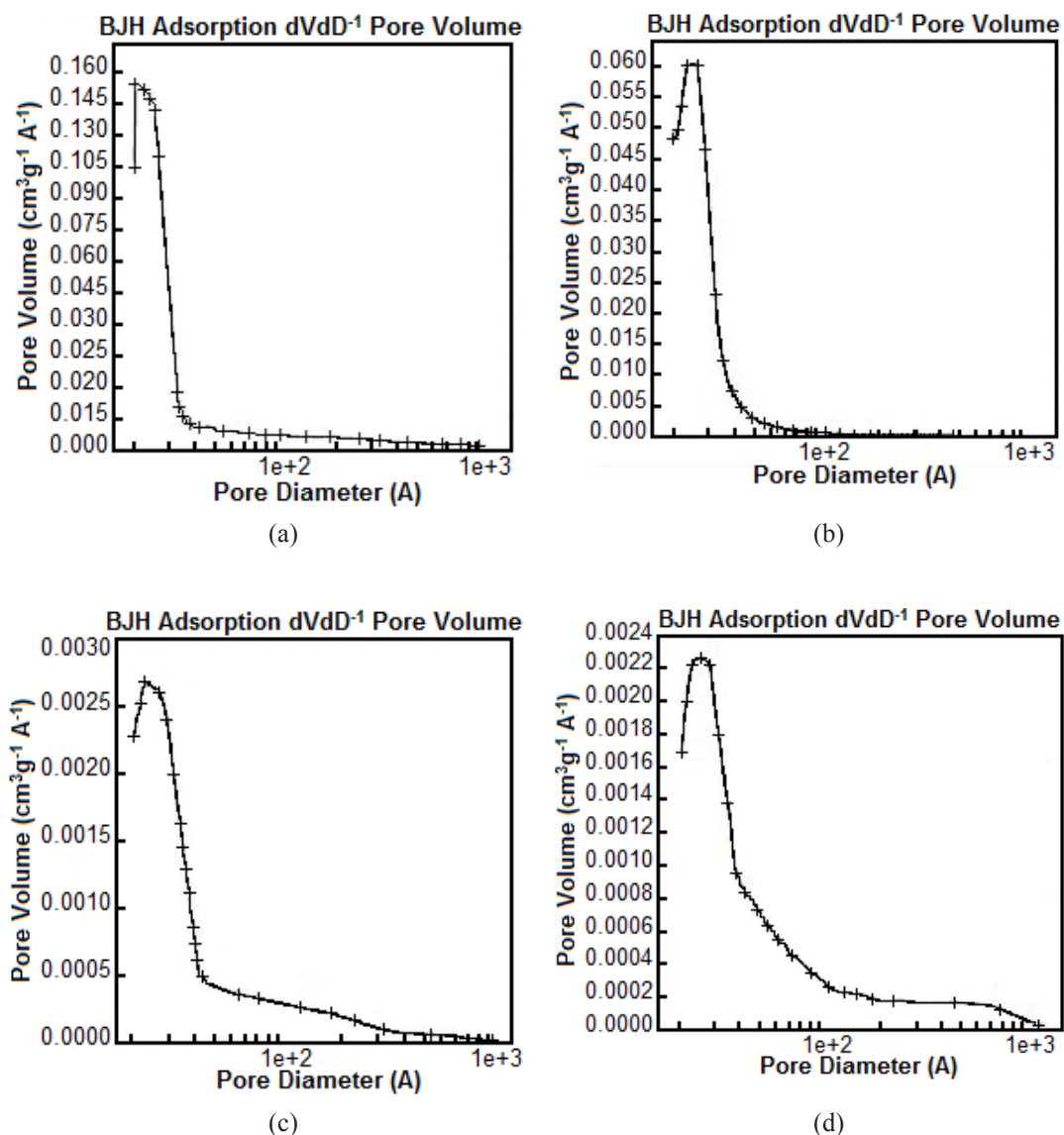


Figure 7: Pore size distribution of (a) Ni MCM-41, (b) Ni MCM-48, (c) Purified MWNTs grew on Ni MCM-41 and (d) purified MWNTs grew on Ni MCM-48.

isotherms corresponding to $p/p_0 < 0.3$ represents the monolayer adsorption of N_2 on the walls of the mesopores, while those with $p/p_0 > 0.4$ represent the multilayer adsorption on the outer surface of the particles. The point at which the reflection begins is related to capillary condensation within the uniform mesopores and their diameter [17,18].

On the other hand, the purified MWNTs that

have been grown on Ni M41S catalysts were characterized by N_2 adsorption, and PSD curves of these samples are shown in Figures 7(c) and 7(d). These results indicate that pore size distribution of grown MWNTs on Ni M41S catalysts follow the pore size distribution of their templates. By comparison of Figure 7(a) and Figure 7(c), it is clear that PSD of purified MWNTs and their Ni MCM41 templates have a large narrow peak between 2-3 nm

and represent similar behavior. This similarity is also observed in the case of MWNTs grown on Ni MCM-48.

Thus by paying attention to the loading of the metal particles during the production process of the mesoporous silicates, the generation of metal particles for CNTs growth with controllable diameter and well-oriented structures was achieved. Controlling the similar metal clusters in the ordered sites of crystalline catalysts was the key point of achieving controlled growth of CNTs. This method was effective for avoiding aggregation of metal particles into large clusters during the high-temperature reaction. This controllable growth of MWNTs causes similarity between the PSDs of the well-ordered grown MWNTs and their silicate framework.

4. CONCLUSIONS

Well-structured mesoporous molecular sieves (MCM-41 and MCM-48) were prepared and Ni particles were loaded on them during the preparation process. With these molecular sieves as the catalysts and acetylene as the carbon precursor, well-graphitized MWNTs were synthesized at 750°C. The CNTs were formed out of the pores of the M41S materials and the maximum yield was greater than 40 wt% of the catalyst. The frameworks of the M41S host materials did not collapse after the synthesis process. By paying attention to the loading of the metal particles during the production process of the mesoporous silicates, generation of metal particles for CNTs growth with controllable diameter and well-oriented structures was achieved. The experimental results indicate that the diameter distribution of the well-ordered grown MWNTs has direct relation with their silicate framework.

REFERENCES

1. Chen, Y.; Ciuparu, D.; Lim, S.; Haller, G. L.; Pfefferle, L. D. The effect of the cobalt loading on the growth of single wall carbon nanotubes by CO disproportionation on Co-MCM-41 catalysts. *Carbon* 2006, 44, 67.
2. Sun, H. D.; Tang, Z. K.; Wang, J. N. Conductance of mono-sized carbon nanotubes in channels of zeolite crystal. *J. Magn. Mater* 1999, 255, 198.
3. Sun, H. D.; Tang, Z. K.; Chen, J.; Li, G. Synthesis and Raman characterization of mono-sized single-wall carbon nanotubes in one-dimensional channels of AlPO₄-5. *Appl. Phys. A* 1999, 69, 381.
4. Tang, Z. K.; Zhang, L. Y.; Wang, N.; Zhang, X. X.; Wen, G. H.; Li, G. D.; Wang, J. N.; Chan, C. T.; Sheng, P. Superconductivity in 4 Angstrom Single-Walled Carbon Nanotubes. *Science* 2001, 292, 2462.
5. Jorio, A.; Souza, A. G. F.; Dresselhaus, G.; Dresselhaus, M. S.; Righi, A.; Matinaga, F. M.; Dantas, M. S. S.; Pimenta, M. A.; Li, Z. M.; Tang, Z. K.; Saito, R. Raman studies on 0.4 nm diameter single wall carbon nanotubes. *Chem. Phys. Lett* 2002, 351, 27.
6. Ryoo, R.; Joo, S. H.; Jun, S. Synthesis of Highly Ordered Carbon Molecular Sieves via Template-Mediated Structural Transformation. *Phys. Chem. B* 1999, 103, 7743.
7. Yang, Y.; Hua, Z.; Lub, Y. N.; Chena, Y. Synthesis of Highly Ordered Carbon Molecular Sieves via Template-Mediated Structural Transformation. *Mat. Chem. Phys* 2003, 82, 440.
8. Liu, Z.; Sakamoto, Y.; Ohsuna, T.; Hirga, K.; Trasaki, O.; Ko, C. H.; Shin, H. J.; Ryoo, R. TEM Studies of Platinum nanowires fabricated in mesoporous silica MCM-41. *Angew. Chem* 2000, 17, 3237.
9. Urban, M.; Mehn, D.; Konya, Z.; Kiricsi, I. Production of carbon nanotubes inside the pores of mesoporous silicates. *Chem. Phys. Lett* 2002, 359, 95.
10. Subashini, D.; Pandurangan, A. Synthesis of mesoporous molecular sieves as catalytic template for the growth of single walled carbon nanotubes Catalysis. *Communications* 2007, 8, 1665.

11. Kaneda, M.; Tsubakiyama, T.; Carlsson, A.; Sakamoto, Y.; Terasaki, Y. O. Structural Study of Mesoporous MCM-48 and Carbon Networks Synthesized in the Spaces of MCM-48 by Electron Crystallography. *J. Phys. Chem. B* 2002, 106, 1256.
12. Williems, I.; Konya, Z.; Fonseca, A.; Nagy, J. B. Heterogeneous catalytic production and mechanical resistance of nanotubes prepared on MgO-supported Co-based catalysts. *Appl. Catal. A* 2002, 229, 229.
13. Colomer, J. F.; Stephan, C.; Lefrant, S.; Tendeloo, G. V.; Konya, I. Z. Large-scale synthesis of single-wall carbon nanotubes by catalytic chemical vapor deposition (CCVD) method. *Chem. Phys. Lett* 2000, 317, 83.
14. Xie, S.; Song, L.; Ci, L.; Zhou, Z.; Dou, X.; Zhou, X.; Sun, G. L. Controllable preparation and properties of single-/double-walled carbon nanotubes. *Sci.Tech. Adv. Mat.* 2005, 6, 725.
15. Kibria, A. K. M. F.; Mo, Y. H.; Nahm, K. S.; Kim, M. J. Synthesis of narrow-diameter carbon nanotubes from acetylene decomposition over an iron–nickel catalyst supported on alumina. *Carbon* 2002, 40, 1241.
16. Kruk, M.; Jaroniec, M. Characterization of Ordered Mesoporous Carbons Synthesized Using MCM-48 Silicas as Templates. *J. Phys. Chem. B* 2000, 104, 7960.
17. Corma, A. From Microporous to Mesoporous Molecular Sieve Materials and Their Use in Catalysis. *Chem. Rev* 1997, 97, 2373.
18. Vinu, A.; Deck, J. D.; Murugasen, V.; Hartmann, M. Synthesis and characterization of CoSBA-1 cubic mesoporous molecular sieves, *Chem. Mater* 2002, 14, 2433.